

We are IntechOpen, the world's leading publisher of Open Access books Built by scientists, for scientists

6,900

Open access books available

185,000

International authors and editors

200M

Downloads

Our authors are among the

154

Countries delivered to

TOP 1%

most cited scientists

12.2%

Contributors from top 500 universities



WEB OF SCIENCE™

Selection of our books indexed in the Book Citation Index
in Web of Science™ Core Collection (BKCI)

Interested in publishing with us?
Contact book.department@intechopen.com

Numbers displayed above are based on latest data collected.
For more information visit www.intechopen.com



Carbon Nanotube Industrial Applications

Fang-Chang Tsai et al*

*Ministry-of-Education Key Laboratory for the Green Preparation and Application of Functional Materials, Faculty of Materials Science and Engineering, Hubei University
China*

1. Introduction

Since carbon nanotube was discovered by S. Iijima in 1991, it has become one of the main academic research subjects. Carbon nanotube is the thinnest tube human can make presently. It has advantages in lightweight, high strength, high toughness, flexibility, high surface area, high thermal conductivity, good electric conductivity and chemical stability. Carbon nanotube can be applied to manufacture smaller transistors or electronic devices. Samsung Korea has made carbon nanotube into Field Emission Display. When the technology is matured and the cost is reduced, it will replace traditional bulky cathode ray tube (CRT) screen. Carbon nanotube has high toughness, so it can be made into high-strength composite with other materials. Thus, carbon nanotube is a material with high economic value and very worth researching. Besides, carbon nanotube has both conductor and semiconductor properties. Therefore, for electronic circuit, the semiconductor property of carbon nanotube enables its application to field emission transistor (FET) gate electrode, which has 100 times higher electric conductivity than silicon semiconductor when voltage is applied and 1000 times higher operational frequency than current Complementary Metal-Oxide Semiconductor (CMOS). The conductor property makes carbon nanotube have similar thermal conductivity to diamond and superior current carrying capacity to copper and gold. For the application of display, its long-term reliability is very excellent [Iijima, 1991, Lee et. al., 1977]. In order to create new material systems with superior properties, various nanoparticle morphologies have been used as reinforcing fillers in elastomeric matrices. These nanometerscale reinforcing particles include spherical particles such as silica or titania [McCarthy et. al., 1997, Kohjiya et. al., 2005], platelets such as layered silicates [Osman et. al., 2001, Joly et. al., 2002, Varghese & Karger-Kocsis, 2003, Kim et. al., 2004, Arroyo et. al., 2003, Bala et. al., 2004, Jeon et. al., 2004], carbon [Gauthier et. al., 2005] or clay fibers [Bokobza & Chauvin, 2005] and multiwall or singlewall carbon nanotubes[Barraza et.

* Chi-Min Shu², Lung-Chang Tsai², Ning Ma¹, Yi Wen¹, Sheng Wen³, Ying-Kui Yang¹, Wei Zhou¹, Han-Wen Xiao¹, Yao-Chi Shu⁴ and Tao Jiang¹

¹Ministry-of-Education Key Laboratory for the Green Preparation and Application of Functional Materials, Faculty of Materials Science and Engineering, Hubei University, China

²Process Safety and Disaster Prevention Laboratory, Department of Safety, Health, and Environmental Engineering, National Yunlin University of Science and Technology, Republic of China

³Faculty of Chemistry and Material Science, Xiaogan University, China

⁴Department of Polymer Materials, Vanung University, Republic of China

al., 2002, López-Manchado et. al., 2004, Hirsch, 2002]. Modified CNTs can enhance the adhesion between CNTs and polymer matrix. Acid modification is one of the most common methods of CNT modification. CNT can be modified by refluxing with nitric acid or a mixture of nitric acid and sulfuric acid. Carboxyl and hydroxyl functional groups are formed on the CNT surface during acid modification [Liu et. al., 2005]. Acid-modified MWCNT can be modified with silane coupling agent [Lee et. al., 2006, Liu et. al., 2005]. The silane will react with the hydroxyl groups ($-OH$) on the surface of MWCNTs. The oxidation of MWCNT may generate carboxylic groups ($-COOH$) rather than hydroxyl groups. Ma et. al. and Vast et. al. suggested that the acid modified MWCNT can generate more hydroxyl groups by reduction process [Ma et. al., 2006 and Vast et. al., 2004]. The development and addition of inorganic and organic moieties into polymer matrix resulted in increasing properties has attracted much interest in the past few years [Liu et. al., 2005, Lee et. al., 2006, Liu et. al., 2005]. Exfoliation is a thermodynamic event that requires compatibility between resin and clay [Vaia & Gianneli, 1977]. Compatibility can be achieved by modifying natural clay using an ion exchange process to replace naturally occurring sodium ions in the gallery between silicate layers with quaternary ammonium ions having organic functionality that render the clay surface hydrophobic [Wen et. al., 2009, Tsai et. al., 2010].

Polyvinyl alcohol (PVA) is low cost, non-toxic, non-polluting, highly transparent, static-interference-free in packaging process, UV resistant and completely biocompatible. Under a dry condition which relative humidity is lower than 50%, PVA and Ethylene Vinyl Alcohol (EVOH) have very good barrier property to effectively block gases and water penetration [Yeh et. al., 2004, Cui et. al., 2009, Okaya et. al., 1992], wear resistance and emulsification ability, and excellent chemical and solvent resistance [Yan, 1998]. However, when the environmental relative humidity is higher than 50% the barrier property for PVA is significantly reduced. Besides, PVA is usually not made into film by hot melt process but by solution process. To improve high-humidity barrier property, PVA is usually treated by capping or crosslinking hydroxyl groups to be less water-absorbing. In recent years, PVA barrier composite film has found applications in food packaging by modifying PVA hydrophobicity and retaining high barrier property. Besides being used as fiber raw material, PVA is largely used in producing coatings, adhesives, paper additives, emulsifiers, dispersants and membranes etc. Its applications spread over textile, food, medicine, construction, wood processing, papermaking, printing, agriculture, steel making and polymer chemicals etc.

In this study, PVA is selected as substrate and mixed-acid and hydrogen peroxide modified carbon nanotube as filler. Mixed acid [Liu et al., 1988] and hydrogen peroxide are first used to treat carbon nanotube by carboxylation to improve its dispersibility. Here, different groups according to different reaction times are investigated to compare among different carboxylation times and carboxylation methods. Then, the carboxylation products are subject to characteristic analysis to learn the effect of reaction condition on the carboxylation degree of CNTs. The modified carbon nanotubes are added to PVA substrate in different mass compositions. The study provides investigation for the first time into the effect of carboxylation method on carbon nanotube structure and property. The result can be used as references for selecting carboxylation method. In the composite aspect, the product comprises water-soluble barrier plastic and conductive filler. The composite retains the performance advantages from both types of materials, such as mechanical properties and electric properties etc. The potential applications for this composite are very versatile, for examples, circuit board with conductive coating, conductive coating on color CRT,

conductive adhesive, nanocarbon conductive coating on electrical grounding network, nanocapacitor, photoelectric conversion device, conductive membrane, antistatic coating, antistatic fiber product and conductive coating plated on non-metal material etc. Better carbon-based electrodes are needed for fuel cells, photocatalyzed water splitting, hydrogen pumps, batteries and other electrocatalytic devices. The requirements for the bulk of fuel cell membranes are mainly high proton conduction, chemical stability and electron insulation. We review the present state of polymer nanocomposites research in which the fillers are carbon nanotubes. In this review, an extended account of the various chemical strategies for grafting polymers onto carbon nanotubes and the manufacturing of carbon nanotube/polymer nanocomposites are given. The thermal analysis and electrical properties to date of a whole range of nanocomposites of various carbon nanotube contents are also reviewed in an attempt to facilitate progress in this emerging area.

2. Modification of carbon nanotubes with polymers

2.1 Materials and sample preparation

The PVA resin and multi-wall carbon nanotube (CNTs) used in this study were obtained from Chang Chun Plastics Co., LTD and Nanotechnologies Port Co., Ltd, Shenzhen, China wherein PVA resin and CNTS had a trade name of 101 L and CNTS is a S.MWNTs-4060. The CCNTs was prepared by sulfuric and nitric mixed acid under ultrasonic vibration. The compositions of the CNTs, CCNTs and PVA / CNTs series specimens prepared in this study are summarized in Table 1, 2 and 3, respectively. According to A series reaction time in Table 1, a proper amount of carbon nanotube is added to mixed acid (concentrated sulfuric acid: concentrated nitric acid = 3: 1).

A series Reaction group	Mixed-acid treatment time (hour)	Hydrogen peroxide treatment time (hour)	B series Reaction group	Mixed-acid treatment time (hour)	Hydrogen peroxide treatment time (hour)
A0	0	0	B0	0	0
A1	1	0	B1	1	0.5
A2	2	0	B2	2	1
A3	4	0	B3	4	2
A4	6	0	B4	6	3
A5	8	0	B5	8	4

Table 1. Formulation for carbon nanotube carboxylation

Ultrasonic vibration is applied according to reaction time. Filtration is conducted with micropore filter and sand core filter. D. I. water is used to rinse the filtrate until it is neutral. The carbon nanotubes from filter are dried in drying oven to obtain a series of mixed-acid modified carbon nanotubes, which are labeled CCNT^{a0} (CNTs), CCNT^{a1}, CCNT^{a2}, CCNT^{a3}, CCNT^{a4} and CCNT^{a5}. Again, according to B series reaction time in Table 1, carbon nanotubes and mixed-acid are treated with ultrasonic vibration and rinsed until it becomes neutral. Then carbon nanotubes are dried in drying oven. The difference with A-series is that hydrogen peroxide ultrasonic vibration treatment is applied to dried carbon nanotube and then the filtrate is rinsed until it becomes neutral. The obtained B series carbon nanotubes are labeled CCNT^{b0} (CNTs), CCNT^{b1}, CCNT^{b2}, CCNT^{b3}, CCNT^{b4} and CCNT^{b5}.

2.2 Observation of carbon nanotube dispersed polarity before and after modification

Six small reagent bottles are added with approximately 6 mL D. I. water and 4 mL toluene and a small amount of carbon nanotubes derived from Table 1. After they are placed in ultrasonic vibrator for 0.5 hours and then, the solution standing storage for 12 hours, they are covered and observed.

2.3 Selection of PVA substrate

Four PVA types are made into solutions of different composition. According to the material property requirements, their electric conductivity and film formation are measured and compared. Then, the one with the highest overall performance is selected as the substrate. After PVA type is decided, eight PVA aqueous solutions are prepared in 1%, 2%, 5%, 6%, 8%, 10%, 12% and 15%. Electric conductivity and aqueous solution stability are used to determine the concentration of PVA aqueous solution as the composite film substrate.

2.4 Preparation of PVA / carbon nanotube composite film

According to the formulations in Table 2 and Table 3, composite film solutions of series-I and series-II are prepared. For series I, 5 groups of CNTs with different carboxylation degree and one unmodified CNTs are used as fillers.

Compositions	PVA (wt%)	CNTs (wt%)
PVA	100.0	0.0
PVA ^{8%_{99.5}} /CCNT ^{b1_{0.5}}	99.5	0.5
PVA ^{8%_{99.5}} /CCNT ^{b2_{0.5}}	99.5	0.5
PVA ^{8%_{99.5}} /CCNT ^{b3_{0.5}}	99.5	0.5
PVA ^{8%_{99.5}} /CCNT ^{b4_{0.5}}	99.5	0.5
PVA ^{8%_{99.5}} /CCNT ^{b5_{0.5}}	99.5	0.5
PVA ^{8%_{99.5}} /CCNT ^{s_{0.5}}	99.5	0.5
CNTs	0.0	100.0

Table 2. Compositions of PVA / CNTs film specimens

They are added in an equal amount into 8% PVA aqueous solutions respectively. By solution blending, they are made into 6 different series I solutions. For series II, CNT^{b5} is used as filler and added 8% PVA aqueous solutions respectively according to formulations in Table 3. Similarly, by solution blending, they are made into 5 different series II solutions. First, weigh the corresponding amount of carbon nanotube into a beaker, add a proper amount of D. I. water, and conduct ultrasonic vibration for 2.5 hours to break apart the agglomerated carbon nanotubes. Weigh the corresponding amount of PVA into the beaker. Place the beaker into a water bath at 80 °C. Agitation is applied by magnetic stirrer for 12 hours to evenly mix carbon nanotubes and PVA. After mixing, transfer the beaker into a heating mantel at about 80 °C to remove excessive solvent – water. In the process, continuous agitation with a glass rod is necessary to prevent formation of a thin layer due to uneven heating. Continue heating and agitation until excessive solvent is removed. Stop when the desired concentration is reached. Keep it still and covered for defoaming. Then, pour the solution into a specially designed mold. Let it dry at room temperature for 12 hours and transfer it to vacuum drier for drying 12 hours. After complete drying, demold to obtain the composite film sample.

Compositions	PVA (wt%)	CNTs (wt%)
PVA	100.0	0.0
PVA ^{8%} _{99.9} /CNT ^{b5} _{0.1}	99.9	0.1
PVA ^{8%} _{99.8} /CNT ^{b5} _{0.2}	99.8	0.2
PVA ^{8%} _{99.5} /CNT ^{b5} _{0.5}	99.5	0.5
PVA ^{8%} _{99.0} /CNT ^{b5} ₁	99.0	1
PVA ^{8%} _{98.0} /CNT ^{b5} ₂	98.0	2
CNTs	0.0	100.0

Table 3. Compositions of PVA / CNTs film specimens

2.5 Fourier transform infrared spectroscopy (FT–IR)

Fourier transform infrared spectroscopic measurements of PVA and PVA/CNTs series specimens were recorded on a Nicolet Avatar 320 FT-IR spectrophotometer at 25°C, wherein 32 scans with a spectral resolution 1 cm⁻¹ were collected during each spectroscopic measurement. Infrared spectra of the film specimens were determined by using the conventional KBr pellet technic.

2.6 Particle size analysis

The particle size analysis measurements of CNTs and CCNTs series specimens were recorded on a Dandong Bettersize Instruments Ltd. BT-9300H at 25 °C and 50 % relative humidity, wherein 6 scans with a 0.1-340 μm were collected during each data measurement. Particle size analysis of powder specimens was determined by using the approximately 15 mL D. I. water and a small amount of carbon nanotubes derived from Table 1.

2.7 Thermal and wide angle X-ray diffraction properties

The thermal properties of PVA and PVA/CNTs series specimens were determined at 25 °C and 50 % relative humidity using a TA Q100 differential scanning calorimetry (DSC), respectively. All scans were carried out at a heating rate of 10°C/min and under flowing nitrogen of a flow rate of 50 mL/min. The instrument was calibrated using pure indium. Samples weighing about 10mg were placed in standard aluminum sample pans for each DSC experiment. The samples were rapidly heated at a heating rate of 40 °C/min and kept at 250 °C for 3 minutes in order to eliminate any residual crystals. The fully melted samples were then cooled at a rate of 10 °C/min, until the crystallization was completed. The melting temperatures of the samples were determined by heating the specimens to 250 °C at a rate of 10 °C/min. The wide angle X-ray diffraction (WAXRD) properties of PVA and PVA/CNTs series specimen diffractometer equipped with a Ni-filtered CuKα radiation operated at 40 kV and 100 mA. Each specimen with 2 mm thickness was maintained stationary and scanned in the reflection mode from 5 to 50° at a scanning rate of 5° /min.

2.8 Measurement of composite film solution conductivity

Use the DJS-1C type platinum black electrode included with the equipment. Prior to measurement, use D. I. water to soak for 24 hours to activate the electrode. Use a thermometer to measure the solution temperature, which is around 23 °C. Switch to CAL and set temperature at 23 °C. According to the electrode constant K=0.952 indicated on electrode cap, adjust the equipment constant to display 952. Now, the equipment set-up is

completed. Use D. I. water to clean the electrode and dry the electrode. Place the electrode into the solution and set the range to 2 ms/cm. Take the reading when it becomes stable. The reading is the electric conductivity for the film solution at 25 °C. After measurement, use D. I. water to clean the electrode and switch the range back to 2 us/cm. When the equipment displays 0, it is ready to measure the next sample. After measurement work is completed, shut off the power, clean the electrode and soak the electrode into D. I. water for next use.

3. Results and discussion

3.1 FT-IR spectral analysis

Figure 1 and Figure 2 summarize FT-IR spectra for all CNTs samples. From the figures, it can be found that absorption band centers for characteristic absorption peaks of CNTs samples are located at 960 and 1645 respectively, referring to bending vibration of hydroxyl group (O-H) of CNTs molecule on different planes and stretching vibration of carboxylate anion. Except that the absorption peak for CNT^{a1} sample is not clear, all other CNTs samples have clear peaks on their spectra.

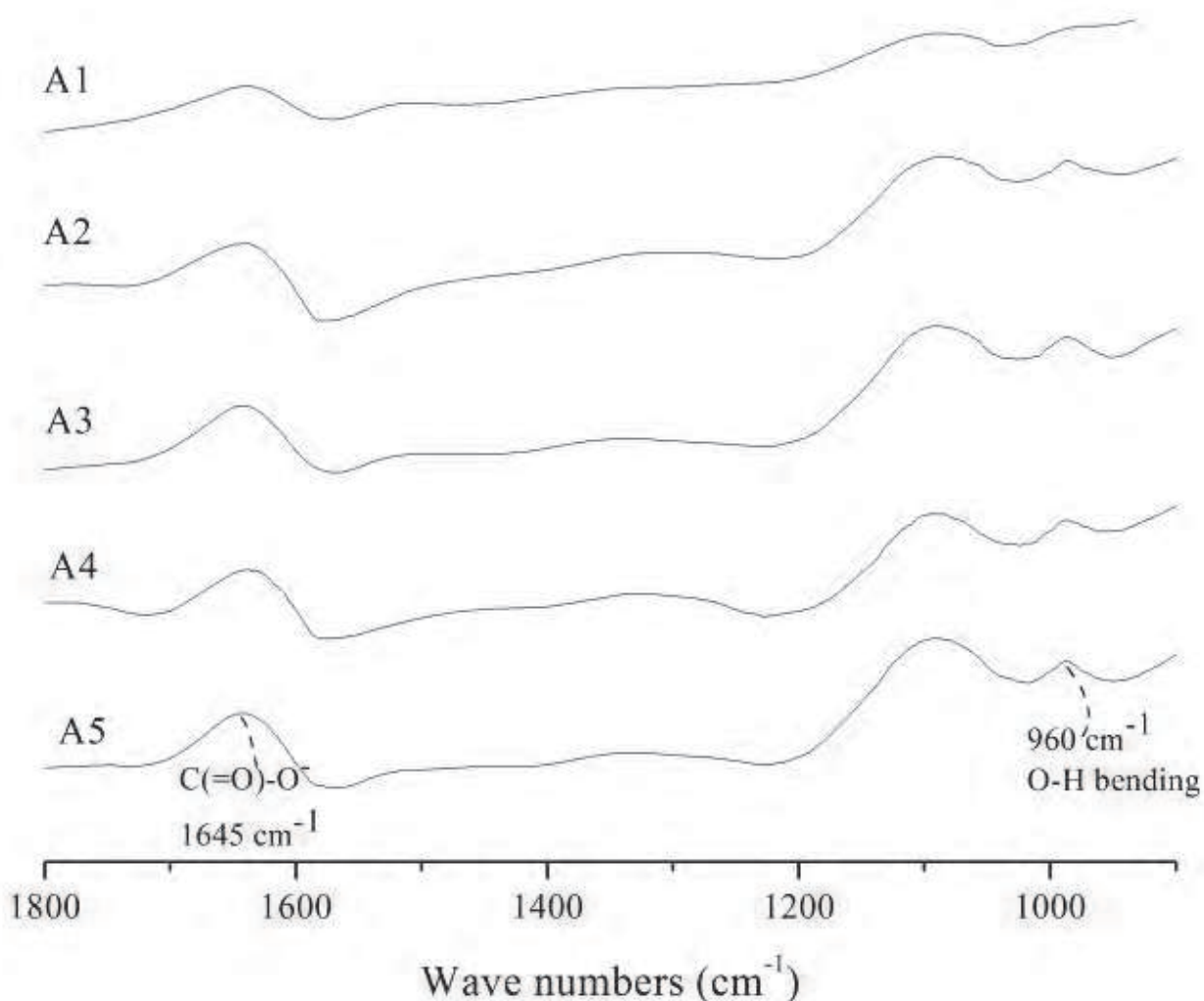


Fig. 1. FT-IR spectra of CCNTs specimens of A-series determined at 25 °C

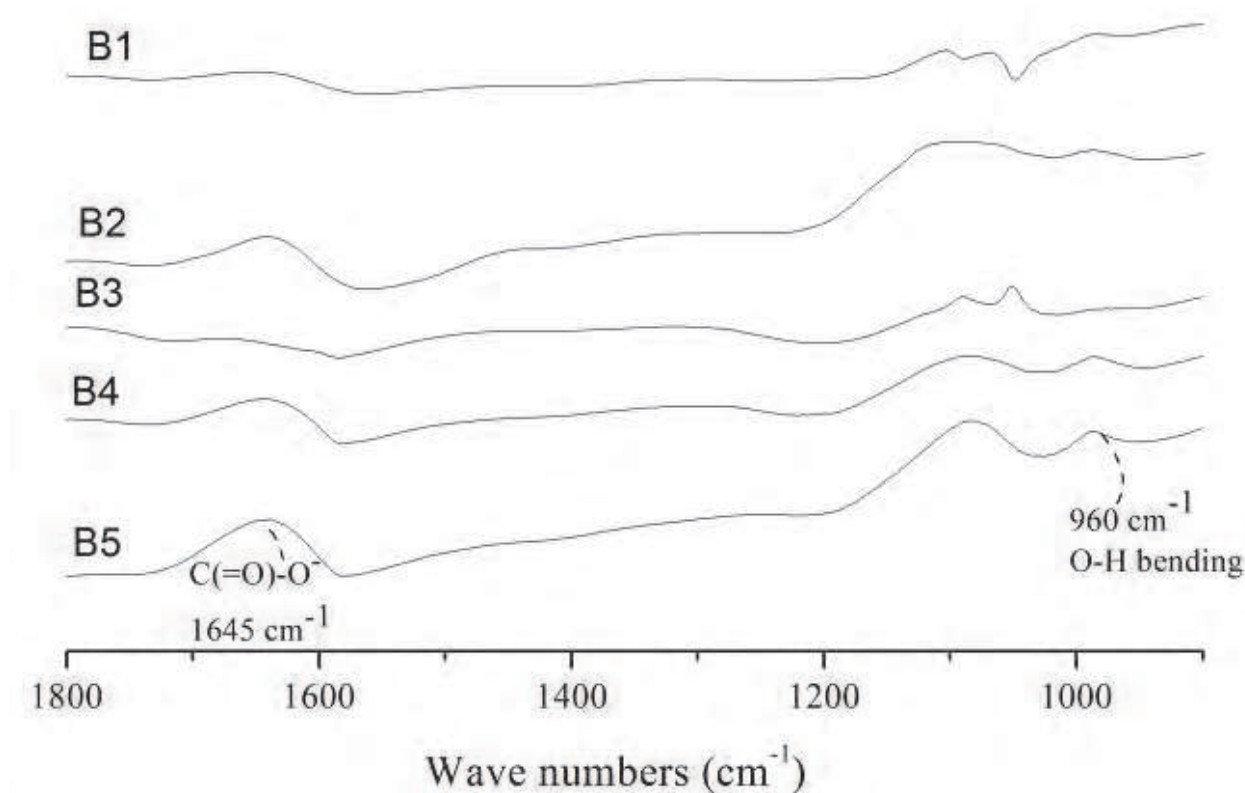


Fig. 2. FT-IR spectra of CCNTs specimens of B-series determined at 25°C

This proves that in Table 1 except A1 all other reaction groups can effectively add carboxyl groups to the carbon nanotubes. After further comparison of the spectra of A series and B series CNTs, it can be found that B series CNTs have stronger absorption peaks than A series CNTs, indicating that the carbon nanotubes treated with mixed-acid, hydrogen peroxide and ultrasonic vibration have more carboxyl groups than the carbon nanotubes treated only with mixed-acid and ultrasonic vibration. The possible carboxylation mechanism on carbon nanotube : mixing concentrated sulfuric acid and concentrated nitric acid generates a large amount of heat; ultrasonic vibration also generates a large amount of heat; the heat facilitates decomposition of concentrated sulfuric acid and release of NO_2 and free oxygen; when two free oxygen atoms and a carbon atom on carbon nanotube combine, it is possible to form a CO_2 and cause carbon nanotube breakage or rupture; the high acidity of the mixed-acid and the strong ultrasonic vibration can also damage and break carbon nanotube; while carbon nanotube becomes thinner, the activity of the carbon atoms on carbon nanotube fracture site increases due to unsaturation; the combination of one oxygen atom and one carbon atom could form a C=O on carbon nanotube and further interact with aqueous H^+ and OH^- and free oxygen to form $-\text{COOH}$ or $-\text{C-OH}$ to generate hydroxyl group; .in the oxidation process, $-\text{COOH}$ and $-\text{OH}$ are usually produced at carbon nanotube end or fracture site, but their quantity is not much.

3.2 Particle size analysis

Particle size analysis is conducted on A-series and B series of carboxylated carbon nanotubes. From Figure 3 and Figure 4, it can be found that with increasing carboxylation reaction time, the extent of carbon nanotube shortening also increases.

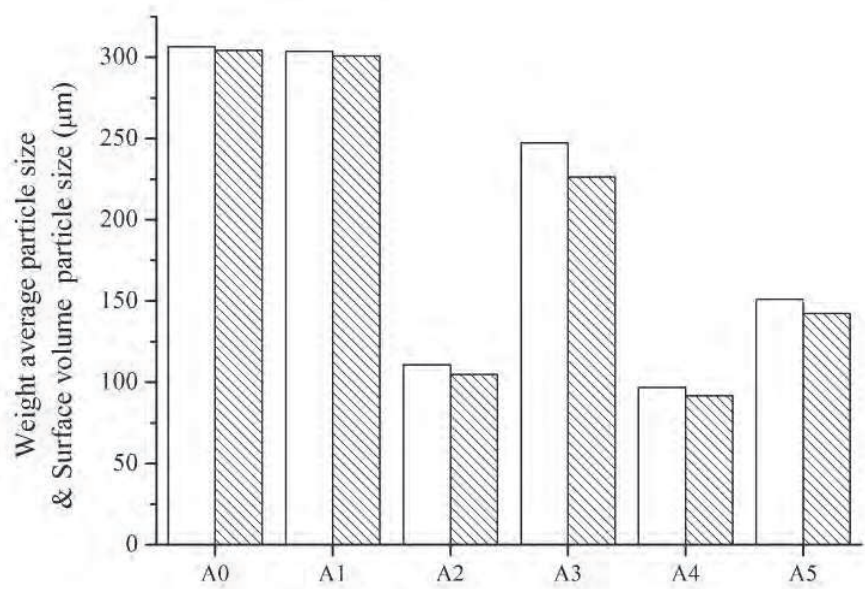


Fig. 3. The A-series of CNTs specimens on weight average particle size (white column) and surface volume particle size (slash column) determined at 25 °C

Particularly in B series, the carbon nanotubes treated with mixed-acid, hydrogen peroxide and ultrasonic vibration basically are all shortened. They are apparently much shorter than A-series of carbon nanotubes treated only with mixed-acid and ultrasonic vibration. This also supports the FT-IR result from a different perspective. The longer the carboxylation reaction time is, the more severe the carbon nanotube is damaged, and the more the rupture on C-C bond the carbon nanotube has. The higher activity at carbon nanotube opening facilitates the bonding with free O and H in water or solution and formation of carboxyl group on fracture site. This can increase the carboxyl functional groups on carbon nanotube and the carboxylation extent for carbon nanotube.

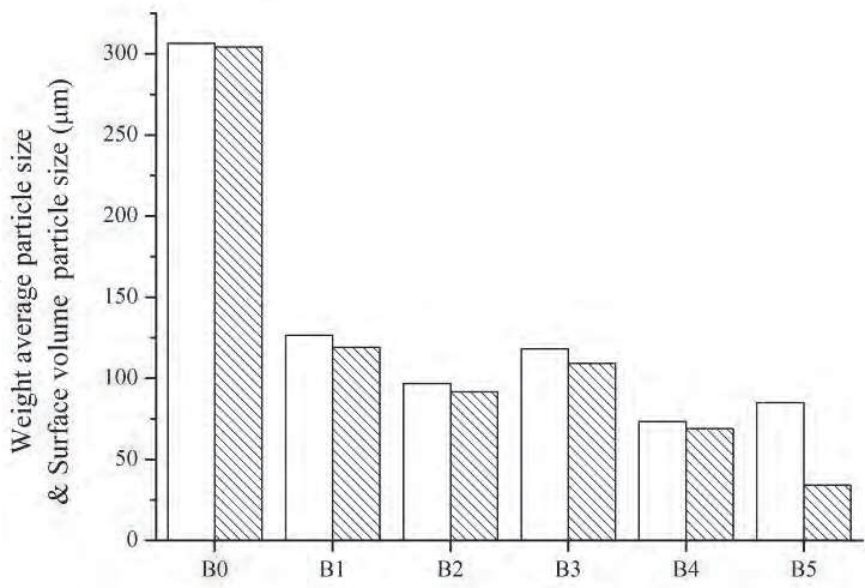


Fig. 4. The B-series of CNTs specimens on weight average particle size (white column) and surface volume particle size (slash column) determined at 25 °C

3.3 Dispersed polarity analysis

Typical photograph of the polarity of CNTs and CCNTs specimens are summarized in Fig. 5. As a result of involves the dispersion state and stability for modified carbon nanotubes in aqueous solution and organic solvent solution. Figure 5 shows the dispersion state for the modified carbon nanotubes in a medium after the treatment in Table1 and being kept still for 12 hours. It can be found from the figure that in the six groups of carbon nanotubes except the unmodified carbon nanotube always existing in the interface of two phases and undissolvable in both phases, all other five groups show different extent of dispersion. Especially, CCNT^{b3} has the most even and stable dispersion in aqueous phase and after being kept still for a week it still maintains the state as in the figure.

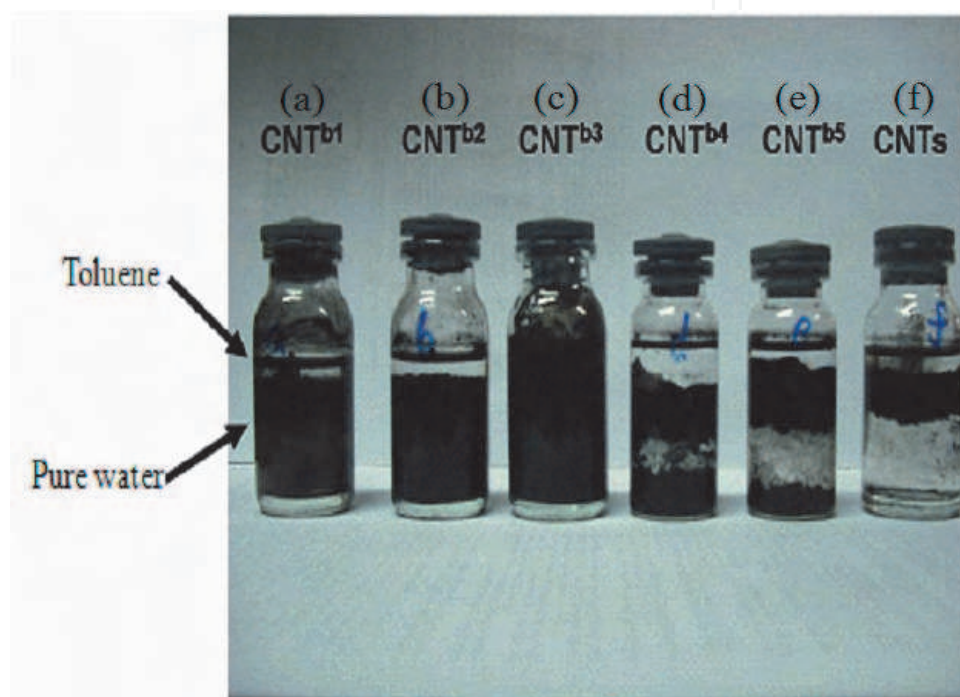


Fig. 5. The photograph of the polarity of pure CNTs specimens

3.4 Selection of PVA type and concentration

The electric conductivities for 3 %, 5 %, 10 % aqueous solutions from A, B, C, D types of PVA are measured and shown in Figure 6. At the same concentration, PVAC has much higher conductivity than the other three. The figure also suggests that the conductivity of PVA solution increases with concentration. The result shown in Figure 7 proves the hypothesis. It shows the conductivities of PVA-C solutions in different concentrations. It can be found that for the aqueous solutions of 1 % - 15 % the conductivity increases with solution concentration. It is worth mentioning that when the concentration reaches above 10 % PVAC solution shows more noticeable gelation and the gel will break up when the temperature increases and show up again when the temperature is back to room temperature. The 8 % PVA aqueous solution is stable without gelation. There is also a reference to indicate 8 % PVA aqueous solution has the most stable viscosity [13] and does not have gelation at room temperature. Gelation will affect significantly product performance. Thus, with consideration of the desired properties for target product, 8 % is the optimal concentration for PVA aqueous solution.

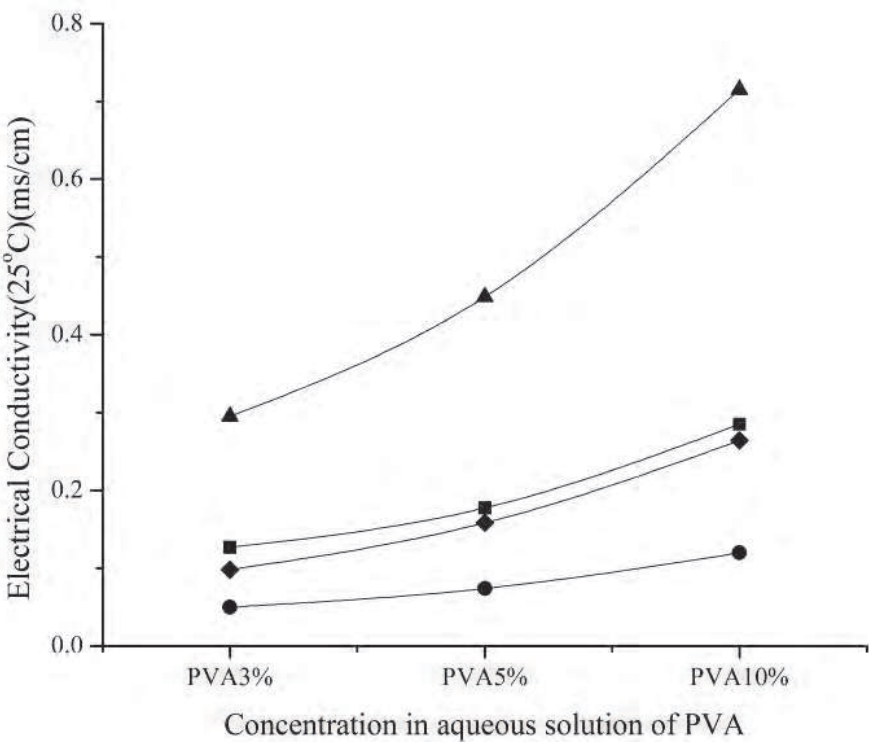


Fig. 6. The electrical conductivities for 3 %, 5 % and 10 % aqueous solutions from A(■), B(●), C(▲), D(◆) types of PVA

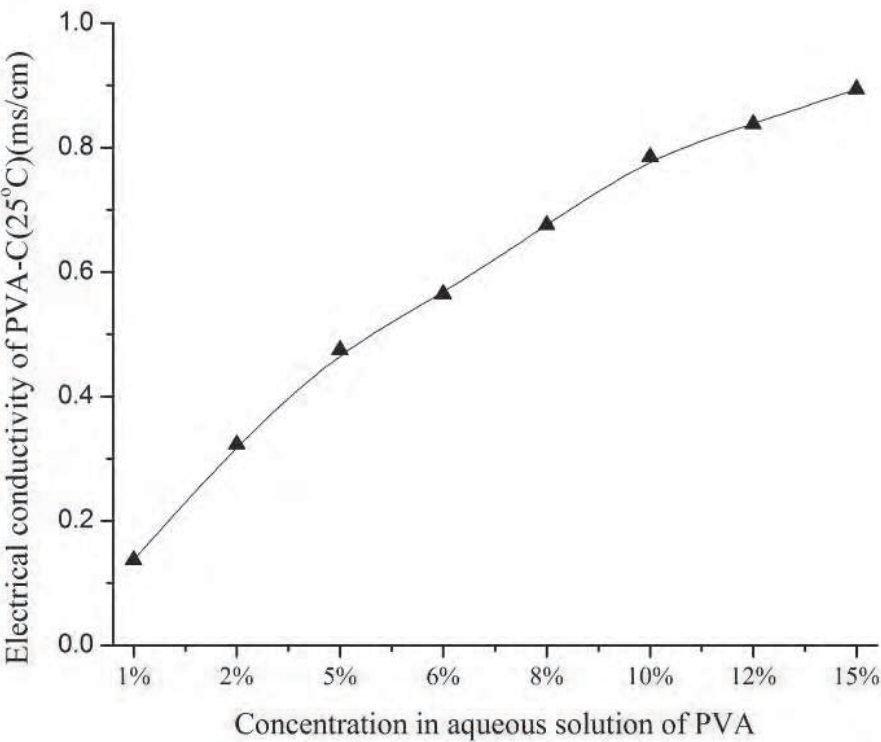


Fig. 7. The electrical conductivities measured at varying concentration in aqueous solutions and 25 °C of PVA^c

The author also conducts draw down to investigate the film forming ability for the four types of PVA. It is conducted on smooth and cleaned glass (by anhydrous ethanol: ether =1: 1) with the PVA solutions of the same concentration. The sample is dried at room temperature and transferred to drying oven at 50 °C for drying until it is completely dried. After the film formation study with 3 % and 5 % PVA aqueous solutions, it is very clear that PVA^C has the best film forming ability and its film has the best stretching property, the best tensile strength and the best demoldability; PVA^D is the second best, and PVA^B and PVA^A perform similarly and not as good as the other two. Based on the consideration of the above two aspects, the final decision is to use 8 % PVA^C aqueous solution as polymer substrate.

3.5 Measurement of electric conductivity for composite films from PVA blended with CNTs of different carboxylation degree

The conductivities for series I films in Table 2 are shown in Figure 8. B0 in the figure represents unmodified CNTs as the control. As shown in the figure, after addition of carbon nanotube the conductivity for composite film solution increases drastically with the carboxylation degree of carbon nanotube. The composite film with carboxylated carbon nanotube has clearly higher electric conductivity than the composite film with unmodified carbon nanotube. Among carboxylated carbon nanotubes, the electric conductivity for the composite films from B1, B2, B3 groups of carbon nanotubes increases with carboxylation degree, but still looks flat without much distinction. It only shows a tendency of increase. However, the composite films from B4, B5 have much higher electric conductivity than the above four groups. Particularly, the carbon nanotube in B5 can achieve the highest electric

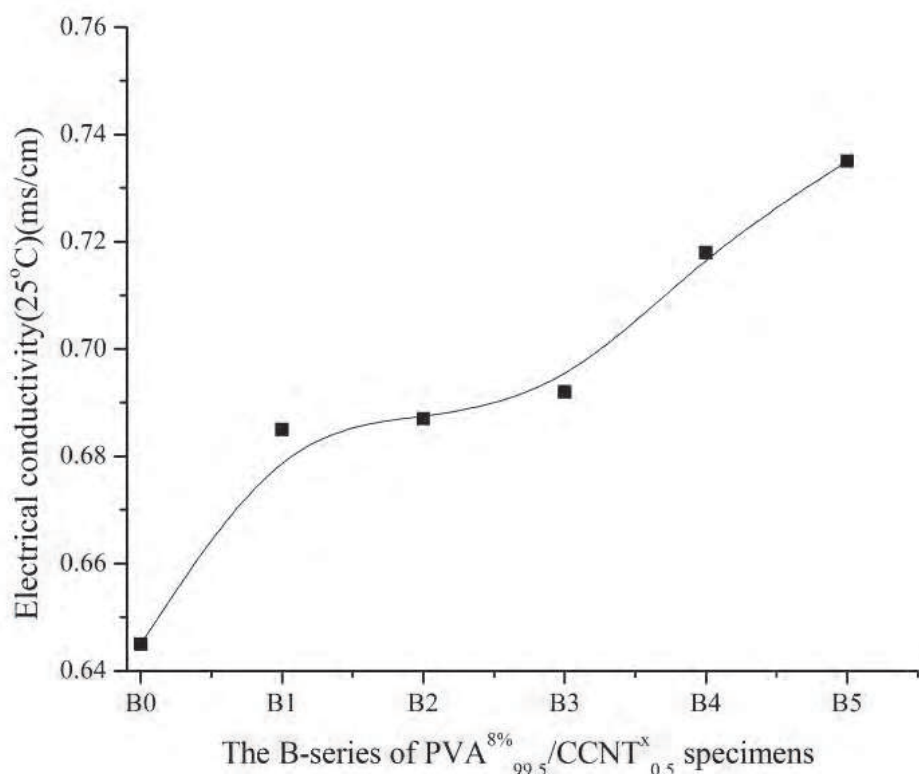


Fig. 8. The B-series of PVA^{8%}_{99.5}/CCNT^x_{0.5} specimens on electrical conductivities determined at 25 °C

conductivity in PVA film solution among all types of carbon nanotubes. From here it can be inferred that the higher the carboxylation degree for carbon nanotube, particularly in this study, the higher the electric conductivity for the composite film is. The hypothesis is that when the carboxylation degree for carbon nanotube is higher, more carbon nanotubes break. The same conclusion can be derived from the particle size analysis result. When the surface hydroxyl groups are more, the carbon nanotube becomes smaller. Since hydroxyl group is hydrophilic and PVA is a water-soluble polymer, in water the more carboxyl groups on carbon nanotube the better affinity with water and the better bonding with PVA. In other words, carbon nanotube will have better dispersibility in PVA substrate. When carbon nanotubes are highly dispersed in every part of PVA molecular framework, it is like adding many conductors to the framework. When carbon nanotubes are added to a certain quantity level, they will form a pseudo conductive network and the composite material will achieve a desirable electric conductivity level.

3.6 Measurement of electric conductivity for composite films from PVA blended with different amount of CNT^{b5}

Figure 9 shows the electric conductivities for PVA film solutions blended with different amount of CCNT^{b5}. It can be found from the figure that in the CCNT^{b5} addition range of 0.1 % - 0.5 % the electric conductivity for composite film increases with increasing addition amount; and in the CCNT^{b5} addition range of 1 % - 2 % the electric conductivity for composite film also increases with increasing addition amount, but less than that in the range of 0.1 % - 0.5 %. Interestingly, in the range of 0.5 % - 1 % the conductivity for composite film solution decreases greatly. Possibly because of insufficient number of composition ratios the trend is not very clear. But it can be anticipated that in the range of 0.5 % - 1 % there will be a composition % for the composite film solution to have the maximum electric conductivity.

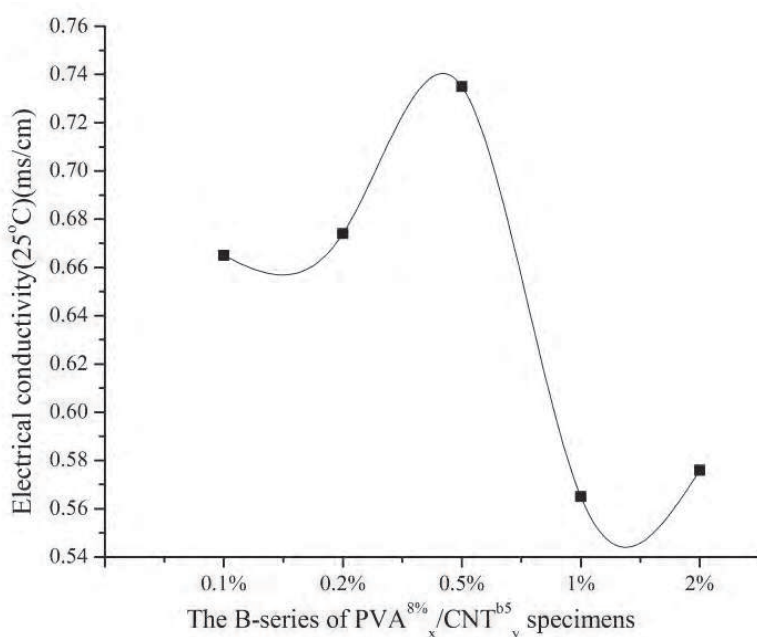


Fig. 9. The B-series of PVA^{8%}/_x/CCNT^{b5}/_y specimens blended with varying amounts CCNT on electrical conductivities determined at 25 °C

3.7 DSC analysis on composite films from PVA blended with different carboxylated CNTs

Figure 10 shows the DSC crystallization curve for the composite films from PVA blended with different carboxylated carbon nanotubes at 0.5 % by weight. It can be found from Figure 10 that addition of carbon nanotube can raise PVA crystallization temperature. Pure PVA has crystallization peak at 193.68 °C. After addition of carbon nanotube, the crystallization peak for all composite films rises to around 203.66 °C of PVA/CNTs and 203.66°C of PVA/CCNTs, respectively. With increasing carboxylation degree for carbon nanotube or increasing damage degree for carbon nanotube, the crystallization peak area for the obtained composite films tends to increase only. It can be inferred that the dispersed carbon nanotubes cause heterogeneous nucleation to PVA crystallization and increase crystallization degree. Due to more perfect crystal, the crystallization temperature for the composite film also increases.

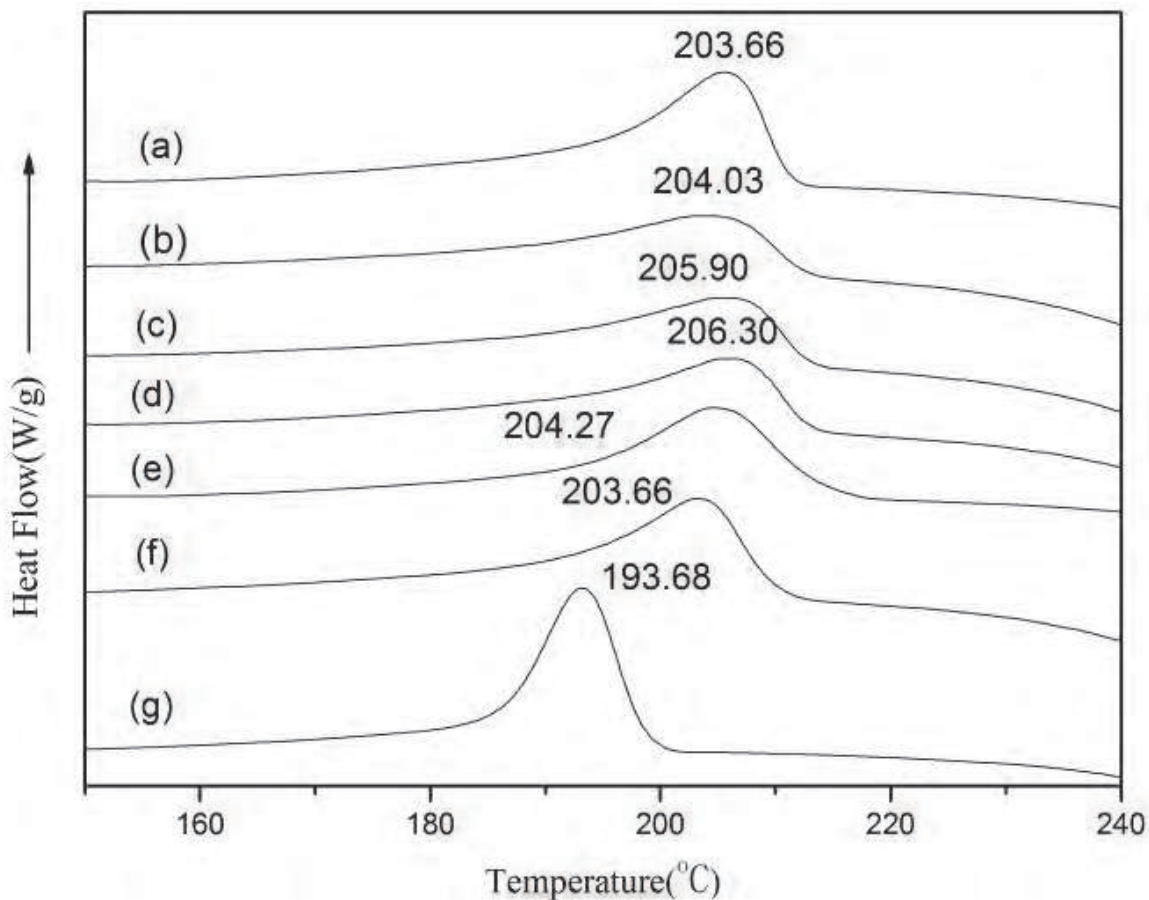


Fig. 10. DSC thermograms of non-isothermal crystallization of (a)PVA^{8%}_{99.5}/CCNT^{b5}_{0.5}, (b) PVA^{8%}_{99.5}/CCNT^{b4}_{0.5}, (c) PVA^{8%}_{99.5}/CCNT^{b3}_{0.5}, (d) PVA^{8%}_{99.5}/CCNT^{b2}_{0.5}, (e) PVA^{8%}_{99.5}/CCNT^{b1}_{0.5}, (f) PVA^{8%}_{99.5}/CCNTs_{0.5} and (g) PVA

Figure 11 shows the melting curve for the composite films from PVA blended with different carboxylation degree of CCNT at 0.5 wt%. Increasing addition of carbon nanotube increases melting temperature for the composite film. For instance, addition of carbon nanotube, the melting temperature for the composite film increases from 218.79 °C for pure PVA to above 224.42 °C of PVA/CNTs and 228.43°C of PVA/CCNTs, respectively.

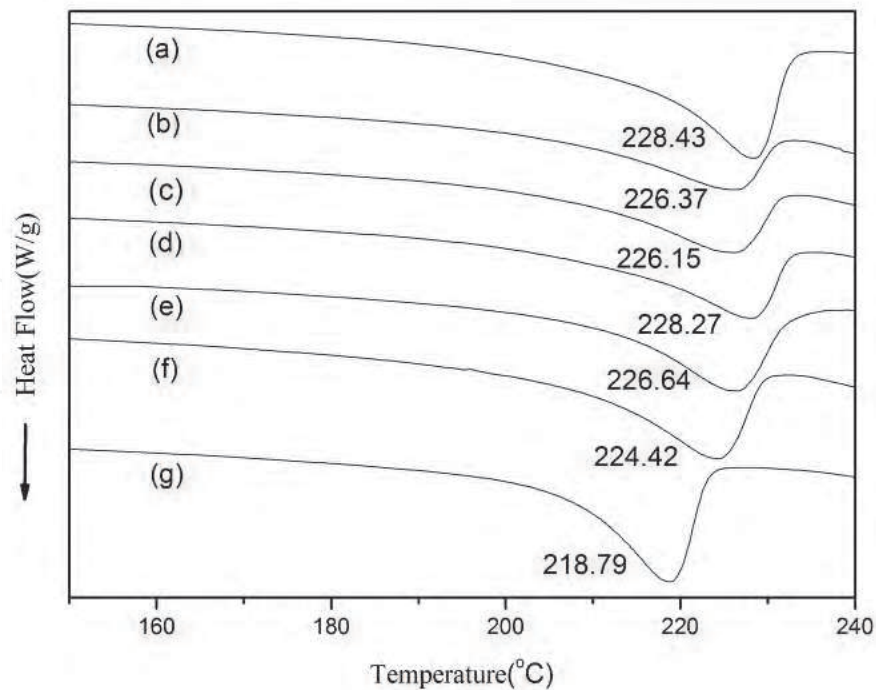


Fig. 11. DSC thermograms of non-isothermal melting of (a)PVA^{8%99.5}/CCNTb⁵_{0.5}, (b) PVA^{8%99.5}/CCNTb⁴_{0.5}, (c) PVA^{8%99.5}/CCNTb³_{0.5}, (d) PVA^{8%99.5}/CCNTb²_{0.5}, (e) PVA^{8%99.5}/CCNTb¹_{0.5}, (f) PVA^{8%99.5}/CCNTs_{0.5} and (g) PVA

Figure 12 shows the DSC crystallization curve for the composite films from PVA aqueous solutions blended with different amount of CCNTb⁵, 0.1 %, 0.2 %, 0.5 %, 1 %, 2 %.

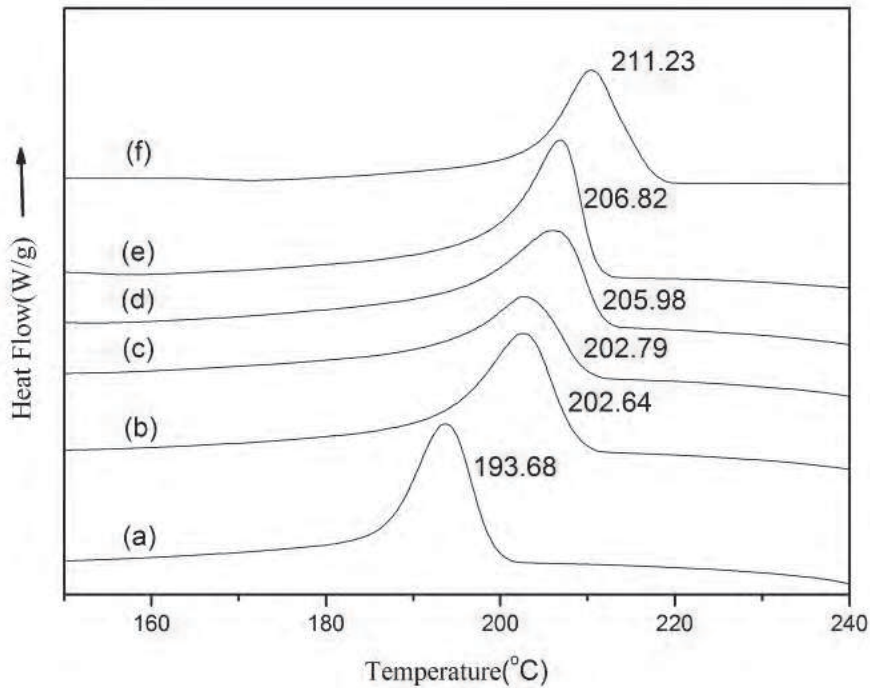


Fig. 12. DSC thermograms of non-isothermal crystallization of (a) PVA, (b) PVA^{8%99.9}/CCNTb⁵_{0.1}, (c) PVA^{8%99.8}/CCNTb⁵_{0.2}, (d) PVA^{8%99.5}/CCNTb⁵_{0.5}, (e) PVA^{8%99.0}/CCNTb⁵₁ and (f) PVA^{8%98.0}/CCNTb⁵₂

Compared to pure PVA, i.e. curve a, the PVA blended with carbon nanotube shows higher crystallization temperature, which supports the hypothesis in previous Section. It can also be found from this figure that the crystallization temperature for the composite film increases with increasing addition of carbon nanotube. In the figure when the composition is PVA^{8%}_{98.0}/CCNT^{b5}₂, the crystallization temperature reaches 211.23 °C and the peak area is the largest. It can be inferred that increasing addition of carbon nanotube can prolong crystallization for PVA composite film and increase crystallization degree. This also means more complete crystallization and more significant heterogeneous nucleation.

Figure 13 shows the melting curve for the composite films from PVA blended with different amount of CCNT^{b5}.

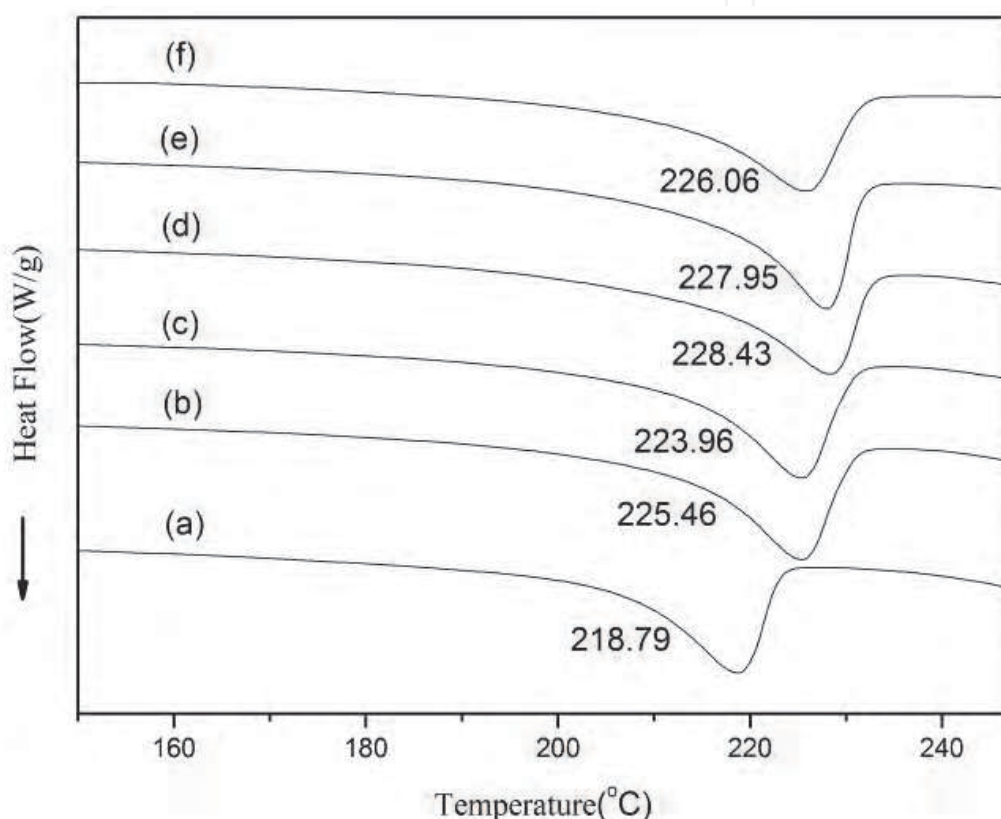


Fig. 13. DSC thermograms of non-isothermal melting of (a) PVA, (b) PVA^{8%}_{99.9}/CCNT^{b5}_{0.1}, (c) PVA^{8%}_{99.8}/CCNT^{b5}_{0.2}, (d) PVA^{8%}_{99.5}/CCNT^{b5}_{0.5}, (e) PVA^{8%}_{99.0}/CCNT^{b5}₁ and (f) PVA^{8%}_{98.0}/CCNT^{b5}₂

Increasing addition of carbon nanotube increases melting temperature for the composite film. With increasing addition of carbon nanotube, the melting temperature for the composite film increases from 218.79 °C for pure PVA to above 228.43°C of PVA^{8%}_{99.5}/CCNT^{b5}_{0.5}. The composite film with more than 0.5% CCNT^{b5} has melting point around 226.06 °C of PVA^{8%}_{98.0}/CCNT^{b5}₂. It can be inferred that with the similar reasoning for Figure 12 the crystallization degree is more complete and the melting point is higher.

3.8 WAXRD analysis

Figure 14 and Figure 15 show the composite films from PVA blended with different carboxylated carbon nanotubes and different amount of CCNT^{b5}.

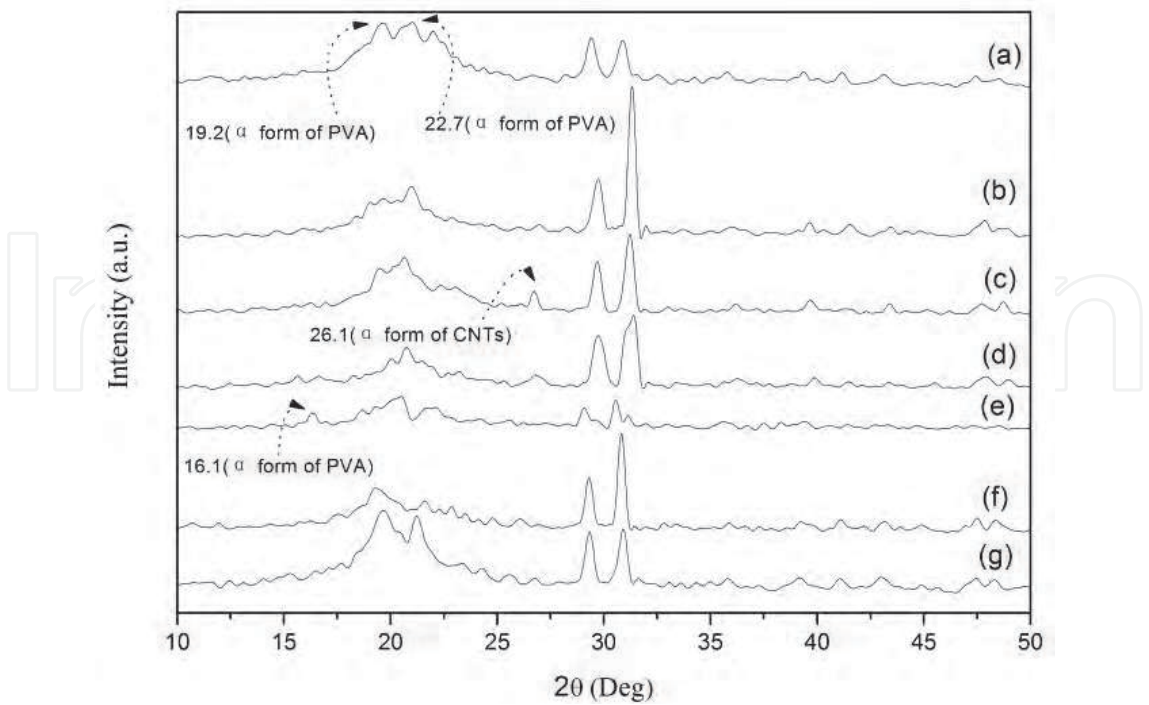


Fig. 14. WAXS diffraction patterns of (a) PVA, (b) PVA^{8%}_{99.5}/CCNT^{b1}_{0.5}, (c) PVA^{8%}_{99.5}/CCNT^{b2}_{0.5}, (d) PVA^{8%}_{99.5}/CCNT^{b3}_{0.5}, (e) PVA^{8%}_{99.5}/CCNT^{b4}_{0.5}, (f) PVA^{8%}_{99.5}/CCNT^{b5}_{0.5} and (g) PVA^{8%}_{99.5}/CNTs_{0.5}

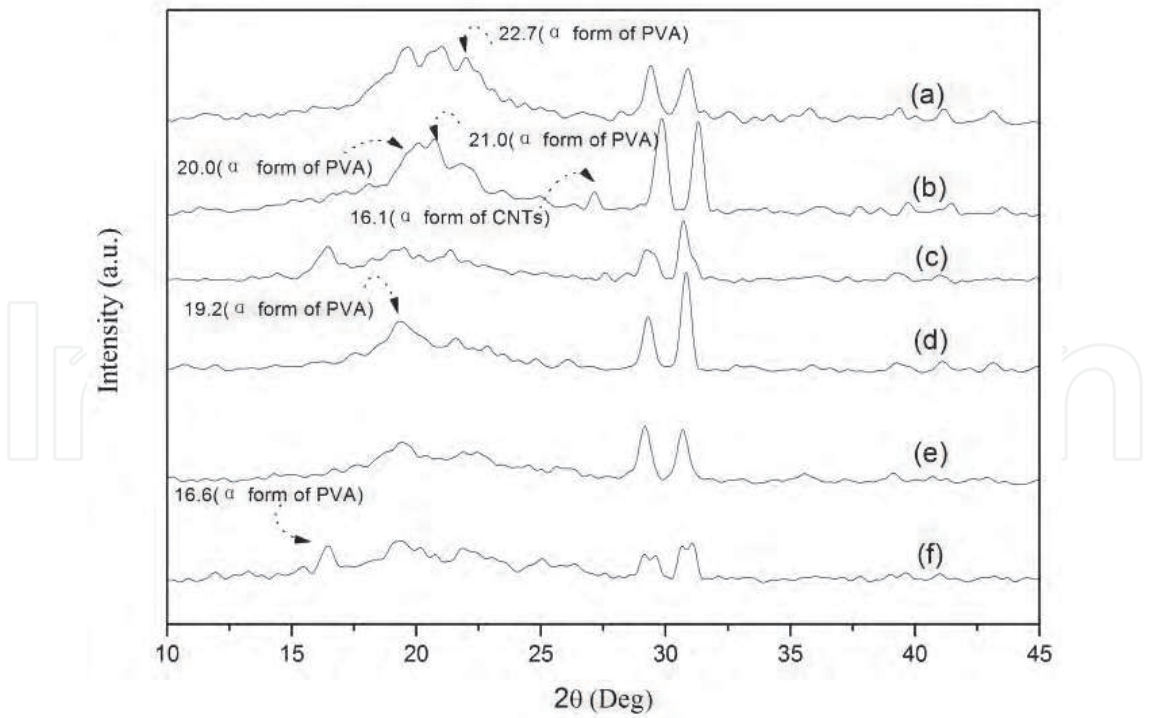


Fig. 15. WAXS diffraction patterns of (a) PVA, (b) PVA^{8%}_{99.9}/CCNT^{b5}_{0.1}, (c) PVA^{8%}_{99.8}/CCNT^{b5}_{0.2}, (d) PVA^{8%}_{99.5}/CCNT^{b5}_{0.5}, (e) PVA^{8%}_{99.0}/CCNT^{b5}₁ and (f) PVA^{8%}_{98.0}/CCNT^{b5}₂

It is consistent with literature values that in the study the X ray diffraction peak angles for the α crystals from PVA samples crystallized from cooling at 25 °C mainly show up at 16.1° , 19.2° , 20.0° , 21.0° and 22.7° ; the XRD peak angle for CNTs sample appears at $2\theta=26.7^\circ$ because the characteristic diffraction peak ^{[14][15]} for crystal plane (002) increases with carboxylation degree. Although the WAXRD diffraction peak for CNTs gradually decreases, their existence is still visible. PVA's diffraction peak levels off. Increasing addition of carbon nanotube decreases the WAXRD diffraction peak for CCNT^{b5} for the composite film. When carbon nanotube is added more than 1 % by weight, CCNT^{b5} peak almost disappears. PVA diffraction peak intensity tends to decrease with increasing addition of carbon nanotube. This proves that carbon nanotube has successfully been blended into PVA substrate and changed PVA crystal morphology. This also supports the projection by DSC that carbon nanotube cause's heterogeneous nucleation in PVA substrate.

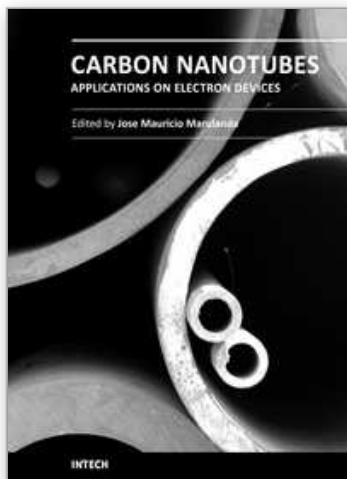
4. Conclusion

In summary, carboxylation for carbon nanotube is an effective solution to improve the dispersibility of carbon nanotubes in polymer. Addition of carbon nanotube into substrate, like PVA, can improve electric property, thermal property and crystal morphology. Carbon nanotube is certainly excellent electrically-conductive and thermally-conductive nano filler for polymers.

5. References

- Iijima, S. (1991). *Nature*, 354, pp. 56.
- Lee, R.S.; Kim, H.J. & Fischer, J.E. (1997). *Nature*, 388, pp. 255.
- McCarthy, D.W.; Mark, J.E. & Schaffer, D.W. (1998). *Journal of Polymer Science, Part B: Polymer Physics*, 36, pp. 1167.
- McCarthy, D.W.; Mark, J.E.; Clarson, S.J. & Schaffer, D.W. (1998). *Journal of Polymer Science, Part B: Polymer Physics*, 36, pp. 1191.
- Kohjiya, S.; Murakami, K.; Iio, S.; Tanahashi, T.; Ikeda, Y.; (2005). *Rubber Chemistry and Technology* 2001, 74, pp. 16.
- Osman, M.A.; Atallah, A. Muller, M. & Suter, U.W. (2001). *Polymer*, 42, pp. 6545.
- Joly, S.; Garnaud, G.; Ollitrault, R. & Bokobza, L. (2002). *Chemistry of Materials*, 14, pp. 4202.
- Varghese, S. & Karger-Kocsis J. (2003). *Polymer*, 44, pp. 4921; (2004). *Rubber World*, 230, pp. 32.
- Kim, J.T.; Oh, T.S. & Lee, D.H. (2004). *Polymer International*, 53, pp. 406.
- Arroyo, M.; Lo'pez-Manchado, M.A. & Herrero, B. (2003). *Polymer*, 44, pp. 2447.
- Bala, P.; Samantaray, B.K.; Srivastava, S.K. & Nando, G.B. (2004). *Journal of Applied Polymer Science* 92, pp.3583.
- Jeon, H.S.; Rameshwaram, J.K. & Kim, G. (2004). *Journal of Polymer Science, Part B: Polymer Physics*, 42, pp. 1000.
- Gauthier, C.; Chazeau, L.; Prasse, T. & Cavaille', J.Y.; (2005). *Composites Science and Technology*, 65, pp. 335.
- Bokobza, L. & Chauvin, J.-P. (2005). *Polymer*, 46, pp. 4144.
- Barraza, H.J.; Pompeo, F.; O'rear, E.A. & Resasco, D.E. (2002). *Nano Letters*, 2, pp. 797.

- Frogle, M.D.; Ravich, D. & Wagner, H.D. (2003). *Composites Science and Technology*, 63, pp. 1647.
- Lo'pez-Manchado, M.A.; Biagiotti, J.; Valentini, L. & Kenny, J.M. (2004). *Journal of Applied Polymer Science*, 92, pp. 3394.
- Hirsch, A. (2002). *Angewandte Chemie International Edition*, 41, pp. 1853-1859
- Ma, P.C.; Kim, J.K. & Tang, B.Z. (2006). *Carbon*, 44, pp. 3232-3238
- Vast, L.; Philippin, G.; Destree, A.; Moreau, N.; Fonseca, A. & Nagy, J.B. (2004). *Nanotechnology*, 15, pp. 781-785.
- Liu, H.; Zhang, W. & Zheng, S. (2005). *J Polym*, 46, pp. 157-165.
- Lee, Y.J.; Kuo, S.W.; Huang, C.F. & Chang, F.C. (2006). *J Polym*, 47, pp. 4378-4386.
- Liu, Y.; Zheng, S. & Nie, K. (2005). *J Polym*, 46, pp. 12016-12025.
- Vaia, R.A. & Giannelis, E.P. (1997). *Macromolecules*, 30, pp. 7990-7999.
- Vaia, R.A. & Giannelis, E.P. (1997). *Macromolecules*, 30, pp. 8000-8009.
- Wen, Y.; Liu, K.; Shang, X.-P.; Tsai, L.-C. & Tsai, F.-C. (2009) "Fabrication and conduction properties of poly(vinyl alcohol) and modified carbon nanotubes blends", 2009 International Workshop on Processing and Properties of Reinforced Polymer Composites, p45.
- Tsai, F.C.; Li, P.; Shang, X.P.; Ma, N.; Tsai, L.C. & Yeh, J.T. (2010). *Advanced Materials Research*, 87-88, pp. 363-368
- Yeh, J. T.; Xu, P. & Tsai, F. C. (2007). *J. Material Sci.*, 42, pp. 6590.
- Cui, L.; Yeh, J.T.; Wang, K.; Tsai, F. C. & Fu, Q. (2009). *J. Memb. Sci.* 327, pp. 226.
- Okaya, T. & Ikari, K. (1992). in *Polyvinyl Alcohol-Developments[C]*, C.A. Finch Ed, at Chapter 8, John Wiley & Sons, New York
- Yan, R. X. (1998). *Water-soluble polymer*, Chemical industry press, Beijing,
- Liu, J.; Rinzler, A. G.; Dai, H.; Hafner, J. H.; Kelley Bradley, R.; Boul, P. J.; Lu, A.; Iverson, T.; Shelimov, K.; Huffman, C. B.; Macias, F. R.; Shon, Y.S.; Lee, T. R.; Colbert, D. T. & Smalley, R. E. (1998). *Science*, 280, pp. 1253.



Carbon Nanotubes Applications on Electron Devices

Edited by Prof. Jose Mauricio Marulanda

ISBN 978-953-307-496-2

Hard cover, 556 pages

Publisher InTech

Published online 01, August, 2011

Published in print edition August, 2011

Carbon nanotubes (CNTs), discovered in 1991, have been a subject of intensive research for a wide range of applications. In the past decades, although carbon nanotubes have undergone massive research, considering the success of silicon, it has, nonetheless, been difficult to appreciate the potential influence of carbon nanotubes in current technology. The main objective of this book is therefore to give a wide variety of possible applications of carbon nanotubes in many industries related to electron device technology. This should allow the user to better appreciate the potential of these innovating nanometer sized materials. Readers of this book should have a good background on electron devices and semiconductor device physics as this book presents excellent results on possible device applications of carbon nanotubes. This book begins with an analysis on fabrication techniques, followed by a study on current models, and it presents a significant amount of work on different devices and applications available to current technology.

How to reference

In order to correctly reference this scholarly work, feel free to copy and paste the following:

Fang-Chang Tsai , Chi-Min Shu, Lung-Chang Tsai, Ning Ma, Yi Wen, Sheng Wen, Ying-Kui Yang, Wei Zhou, Han-Wen Xiao, Yao-Chi Shu and Tao Jiang (2011). Carbon Nanotube Industrial Applications, Carbon Nanotubes Applications on Electron Devices, Prof. Jose Mauricio Marulanda (Ed.), ISBN: 978-953-307-496-2, InTech, Available from: <http://www.intechopen.com/books/carbon-nanotubes-applications-on-electron-devices/carbon-nanotube-industrial-applications>

INTECH
open science | open minds

InTech Europe

University Campus STeP Ri
Slavka Krautzeka 83/A
51000 Rijeka, Croatia
Phone: +385 (51) 770 447
Fax: +385 (51) 686 166
www.intechopen.com

InTech China

Unit 405, Office Block, Hotel Equatorial Shanghai
No.65, Yan An Road (West), Shanghai, 200040, China
中国上海市延安西路65号上海国际贵都大饭店办公楼405单元
Phone: +86-21-62489820
Fax: +86-21-62489821

© 2011 The Author(s). Licensee IntechOpen. This chapter is distributed under the terms of the [Creative Commons Attribution-NonCommercial-ShareAlike-3.0 License](https://creativecommons.org/licenses/by-nc-sa/3.0/), which permits use, distribution and reproduction for non-commercial purposes, provided the original is properly cited and derivative works building on this content are distributed under the same license.

IntechOpen

IntechOpen